Three-dimensional soil moisture profile retrieval by assimilation of near-surface measurements: Simplified Kalman filter covariance forecasting and field application

Jeffrey P. Walker,[1] Garry R. Willgoose, and Jetse D. Kalma

Department of Civil, Surveying and Environmental Engineering, University of Newcastle, Callaghan, New South Wales, Australia

Received 1 July 2002; revised 1 August 2002; accepted 1 August 2002; published 19 December 2002.

[1] The Kalman filter data assimilation technique is applied to a distributed three-dimensional soil moisture model for retrieval of the soil moisture profile in a 6 ha catchment using near-surface soil moisture measurements. A simplified Kalman filter covariance forecasting methodology is developed based on forecasting of the state correlations and imposed state variances. This covariance forecasting technique, termed the modified Kalman filter, was then used in a 1 month three-dimensional field application. Two updating scenarios were tested: (1) updating every 2 to 3 days and (2) a single update. The data used were from the Nerrigundah field site, near Newcastle, Australia. This study demonstrates the feasibility of data assimilation in a quasi three-dimensional distributed soil moisture model, provided simplified covariance forecasting techniques are used. It also identifies that (1) the soil moisture profile cannot be retrieved from near-surface soil moisture measurements when the near-surface and deep soil layers become decoupled, such as during extreme drying events; (2) if simulation of the soil moisture profile is already good, the assimilation can result in a slight degradation, but if the simulation is poor, assimilation can yield a significant improvement; (3) soil moisture profile retrieval results are independent of initial conditions; and (4) the required update frequency is a function of the errors in model physics and forcing data. *INDEX TERMS:* 1866 Hydrology: Soil moisture; 1875 Hydrology: Unsaturated zone; 1894 Hydrology: Instruments and techniques; *KEYWORDS:* soil moisture, remote sensing, data assimilation, catchment hydrology, field study, covariance estimation

Citation: Walker, J. P., G. R. Willgoose, and J. D. Kalma, Three-dimensional soil moisture profile retrieval by assimilation of near-surface measurements: Simplified Kalman filter covariance forecasting and field application, *Water Resour. Res.*, *38*(12), 1301, doi:10.1029/2002WR001545, 2002.

1. Introduction

[2] An ability to retrieve the soil moisture profile for a one-dimensional soil column by assimilation of near-surface soil moisture measurements using the Kalman filter (KF) has been demonstrated in one-dimensional synthetic studies [e.g., *Entekhabi et al.*, 1994; *Galantowicz et al.*, 1999; *Hoeben and Troch*, 2000; *Walker et al.*, 2001a; *Walker and Houser*, 2001; *Reichle et al.*, 2002] and one-dimensional field applications [e.g., *Galantowicz et al.*, 1999; *Walker et al.*, 2001b]. However, the one-dimensional nature of these studies has restricted the application of this work to saturation excess catchments, where lateral flow and thus spatial coupling is known to be a dominant physical process. Critical challenges in this spatially coupled problem include the lack of adequate spatially distributed field data and the computational demands of applying the KF within a distributed model. This paper, the third in a series on hydrologic data assimilation, presents a simplified KF covariance forecasting approach to the distributed problem, thus making the distributed covariance forecasting problem computationally tractable, and demonstrates its use in a catchment scale field application using a distributed soil moisture model.

[3] System state covariance forecasting is widely recognized as being the most computationally expensive aspect of the KF algorithm [*Dee*, 1991; *Todling and Cohn*, 1994; *Dee*, 1995], with system state covariance forecasting costing roughly $2N$ times (where N is the number of system states) the cost of the mean system state forecast [*Dee*, 1991]. The cost of covariance forecasting is such that implementation of the KF as a scheme for data assimilation by "brute-force" is recognized as being unfeasible for large systems because of both its extensive computational requirements and a lack of complete knowledge of its required statistical inputs [*Todling and Cohn*, 1994]. Computational requirements for the updating step of the KF are less severe but nontrivial.

[4] *Todling and Cohn* [1994] noted that the lack of complete information concerning statistics of model errors, and even observation errors, makes the effort of evolving the complete forecast covariance matrix as dictated by the KF not worthwhile. Furthermore, as a consequence of the

[1] Now at Department of Civil and Environmental Engineering, University of Melbourne, Parkville, Victoria, Australia.

0043-1397/02/2002WR001545$09.00

assumptions in the KF and the linearization of state forecasting equations, even a full-fledged application of the extended KF can only roughly approximate the actual system state covariance evolution [*Dee*, 1991, 1995].

[5] Accordingly, we view the covariance forecasting equation as simply a means for representing the forecast covariances, which approximately accounts for the effects of error propagation by the forecast model as well as for additional effects of model error. It follows that other approximations for the KF forecast covariance evolution can be legitimately introduced, particularly in the computationally expensive propagation term [*Dee*, 1995].

[6] A number of alternatives for estimating the forecast covariance matrix have been presented in the literature and are reviewed by *Todling and Cohn* [1994]. They divided these simplified covariance estimation schemes into six main categories: (1) Covariance modeling assumes a specified form for the forecast covariance matrices, with no dynamics of these matrices taken into account. (2) Dynamics simplification uses approximate system state dynamics to evolve the forecast covariances. (3) Reduced resolution decreases the dimensionality of the problem by computing the forecast covariances with a coarser resolution model than the model used to forecast the states. A hybrid of the dynamics simplification and reduced resolution schemes may also be considered. (4) Local approximation evolves the forecast covariance structure only for points separated by reasonably small distances. (5) Limiting filtering computes a fixed gain matrix and an asymptotic system state covariance structure. (6) Monte Carlo methods estimate the forecast covariance matrix by integrating an ensemble of states between observation times.

[7] Previous work by the authors has demonstrated a computationally feasible methodology for one-dimensional soil moisture assimilation, firstly with synthetic data [*Walker et al.*, 2001a], and then using field data [*Walker et al.*, 2001b]. This paper extends the previous work to situations where lateral flows are important and spatial coupling of soil moisture must be considered. The spatial coupling necessitated development of a computationally efficient methodology for forecasting the system state covariances. The approach taken is based on dynamics simplification, but we don't derive simplified model dynamics for the covariance forecasting. The same model physics used for state forecasting are used for the covariance forecasting procedure, except that we forecast only the correlation between the states and impose the standard deviations based on observed model fit to data without data assimilation.

2. Soil Moisture Model

[8] A schematic of the distributed soil moisture model used in this paper is given in Figure 1. Layer 1 is of constant thickness over the entire catchment and would be set commensurate with the approximate remote sensing observation depth [*Walker et al.*, 1997] when used in a remote sensing application. At least one additional layer is modeled to represent the remaining soil profile. As soil depth is spatially variable, the lower layer(s) are of varying thickness in order to maintain the same number of soil layers throughout the model domain. Thus layer thickness is modeled as a fixed proportion of the soil depth.

[9] Unsaturated flow through porous media is modeled by the Buckingham-Darcy equation as

$$Q = K\nabla(\psi + z), \tag{1}$$

where Q is the volumetric flux of liquid water, positive downward, K is the unsaturated hydraulic conductivity, ∇ is the gradient operator, ψ is the matric suction and z is the elevation, positive downward. Using the approximation of *Walker et al.* [2001b], the soil moisture fluxes in the vertical (perpendicular to soil surface) and lateral (parallel to soil surface) directions respectively are

$$Q_V = K \cdot VDF + K \cdot (1 - SLOPE) \tag{2a}$$

$$Q_L = K \cdot LDF + K \cdot SLOPE, \tag{2b}$$

where the vertical (VDF) and lateral (LDF) distribution factors for grid element j,k,l are given by

$$VDF = GRAD_{j+1/2,k,l}\left(\frac{\theta_{j,k,l} - \theta_{r_{j,k,l}}}{\phi_{j,k,l} - \theta_{r_{j,k,l}}} - \frac{\theta_{j+1,k,l} - \theta_{r_{j+1,k,l}}}{\phi_{j+1,k,l} - \theta_{r_{j+1,k,l}}}\right) \tag{3a}$$

$$LDF = GRAD_{j,k+1/2,l}\left(\frac{\theta_{j,k,l} - \theta_{r_{j,k,l}}}{\phi_{j,k,l} - \theta_{r_{j,k,l}}} - \frac{\theta_{j,k+1,l} - \theta_{r_{j,k+1,l}}}{\phi_{j,k+1,l} - \theta_{r_{j,k+1,l}}}\right), \tag{3b}$$

and

$$GRAD_{j+1/2,k,l} = \frac{0.5}{DZ}\left(\frac{MGRAD_{j,k,l} + MGRAD_{j+1,k,l}}{\left(\theta_{j,k,l} - \theta_{r_{j,k,l}}\right)^2 + \left(\theta_{j+1,k,l} - \theta_{r_{j+1,k,l}}\right)^2}\right) \tag{4a}$$

$$GRAD_{j,k+1/2,l} = \frac{0.5}{DX}\left(\frac{MGRAD_{j,k,l} + MGRAD_{j,k+1,l}}{\left(\theta_{j,k,l} - \theta_{r_{j,k,l}}\right)^2 + \left(\theta_{j,k+1,l} - \theta_{r_{j,k+1,l}}\right)^2}\right). \tag{4b}$$

$MGRAD$ is the maximum matric suction gradient for a unit change in moisture content [*Walker et al.*, 2001b], θ is the volumetric soil moisture, ϕ is the soil porosity, θ_r is the residual soil moisture content, DZ is the perpendicular distance between the midpoints of layer j and $j + 1$ and DX is the lateral slope distance between the midpoints of grid cell k,l and $k + 1,l$. $SLOPE$ is the topographic slope between the midpoints of the soil layer (m m^{-1}) in the drainage direction (maximum downslope direction), however, for simplicity, it may be taken as the surface slope. This simplification avoids the possibility of different layers in the same grid cell draining to different grid cells. Hence, the soil moisture model is a quasi three-dimensional model, with redistribution of soil moisture only occurring in two directions for any given grid element, i.e., vertically and laterally in the maximum downslope direction.

[10] Substitution of (3) and (4) in (2) yields the vectorized soil moisture flux equations:

$$Q_{V_{j,k,l}} = \left\langle \frac{GRAD_{j+1/2,k,l} \cdot K_{j+1/2}, k, l}{\left(\phi_{j,k,l} - \theta_{r_{j,k,l}}\right)}, -\frac{GRAD_{j+1/2,k,l} \cdot K_{j+1/2,k,l}}{\left(\phi_{j+1,k,l} - \theta_{r_{j+1,k,l}}\right)} \right\rangle \begin{Bmatrix} \theta_{j,k,l} \\ \theta_{j+1,k,l} \end{Bmatrix} + \left\langle \begin{matrix} K_{j+1/2,k,l} \cdot (1 - SLOPE) - \\ GRAD_{j+1/2,k,l} \cdot K_{j+1/2,k,l}\left(\frac{\theta_{r_{j,k,l}}}{\phi_{j,k,l} - \theta_{r_{j,k,l}}} + \frac{\theta_{r_{j+1,k,l}}}{\phi_{j+1,k,l} - \theta_{r_{j+1,k,l}}}\right) \end{matrix} \right\rangle \tag{5a}$$

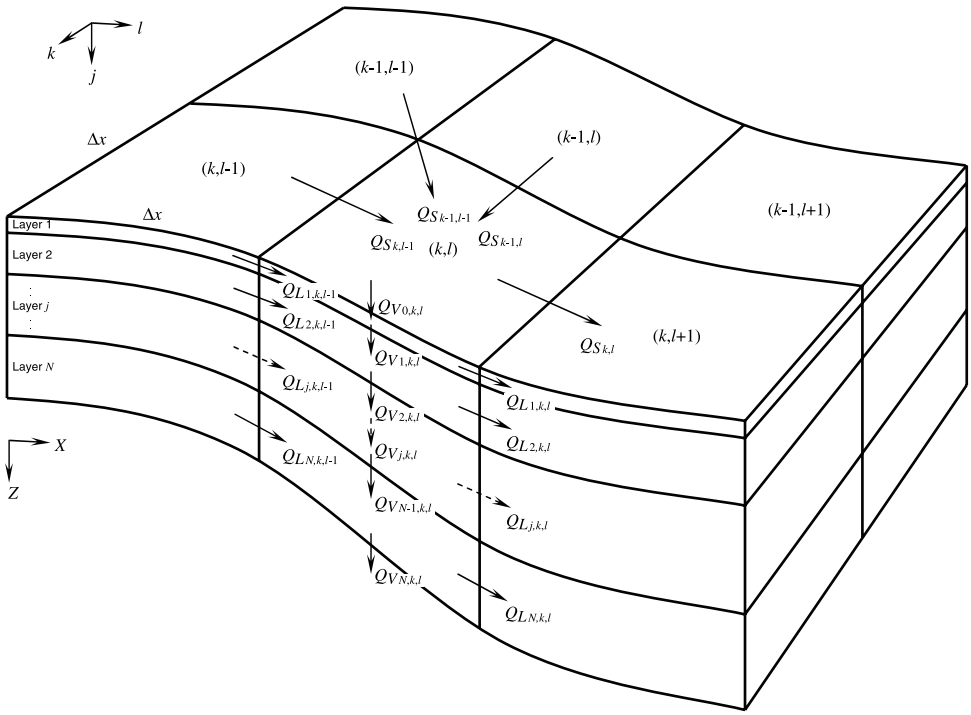

Figure 1. Schematic representation of the distributed soil moisture model.

$$Q_{L_{j,k,l}} = \left\langle \frac{GRAD_{j,k+1/2,l} \cdot K_{j,k+1/2,l}}{\left(\phi_{j,k,l} - \theta_{r_{j,k,l}}\right)}, -\frac{GRAD_{j,k+1/2,l} \cdot K_{j,k+1/2,l}}{\left(\phi_{j,k+1,l} - \theta_{r_{j,k+1,l}}\right)} \right\rangle \begin{Bmatrix} \theta_{j,k,l} \\ \theta_{j,k+1,l} \end{Bmatrix} + \left\langle \begin{matrix} K_{j,k+1/2,l} \cdot SLOPE - \\ GRAD_{j,k+1/2,l} \cdot K_{j,k+1/2,l} \left(\frac{\theta_{r_{j,k,l}}}{\phi_{j,k,l} - \theta_{r_{j,k,l}}} + \frac{\theta_{r_{j,k+1,l}}}{\phi_{j,k+1,l} - \theta_{r_{j,k+1,l}}} \right) \end{matrix} \right\rangle, \quad (5b)$$

where the intermediate hydraulic conductivities are calculated as the arithmetic means.

[11] Applying continuity in both the vertical and lateral directions and the Crank-Nicholson scheme [*Gerald and Wheatley*, 1989] yields the implicit forecast equation

$$\theta_{j,k,l}^{n+1} - \frac{1}{2} \left(\begin{matrix} \left[Q_{V_{j-1,k,l}} - Q_{V_{j,k,l}}\right] \frac{\Delta t}{\Delta z} \\ + \left[Q_{L_{j,k,l-1}} - Q_{L_{j,k,l}}\right] \frac{\Delta t}{\Delta x} \end{matrix} \right)^{n+1} = \theta_{j,k,l}^{n} + \frac{1}{2} \left(\begin{matrix} \left[Q_{V_{j-1,k,l}} - Q_{V_{j,k,l}}\right] \frac{\Delta t}{\Delta z} \\ + \left[Q_{L_{j,k,l-1}} - Q_{L_{j,k,l}}\right] \frac{\Delta t}{\Delta x} \end{matrix} \right)^{n}. \quad (6)$$

Substituting the soil moisture flux equations from (5) and assembling the soil moisture state equation in matrix form we obtain

$$\Phi_1^{n+1} \cdot \hat{\mathbf{X}}^{n+1/n} + \Omega_1^{n+1} = \Phi_2^{n} \cdot \hat{\mathbf{X}}^{n/n} + \Omega_2^{n}, \quad (7)$$

where Φ is the matrix of coefficients for the vector of moisture values $\mathbf{X}$ and Ω is the vector of nonmoisture dependent terms. The notation $n + 1/n$ is used to identify a forecast at time step $n + 1$ given the forecast at time step n. As (7) is an implicit equation, iteration is required until convergence is obtained for each time step. The advantage of writing the soil moisture equation in an implicit form rather than an explicit form, as traditionally used in KF covariance forecasting, is that much larger time steps may be made, allowing the model to run much more quickly than the explicit form.

[12] The lateral soil moisture flux at the catchment outlet is estimated by assuming that only gravity drainage occurs (i.e., zero lateral moisture gradient), as there is no knowledge of the soil moisture content of the downhill grid cell. Moreover, the soil moisture content at the catchment outlet is often high, meaning that capillary effects will be minimal.

[13] The mass balance for each of the grid elements is ensured by upwelling any forecast soil moisture storage in excess of the soil porosity to the soil layer above. Starting from the lowest soil layer in each grid cell, this procedure is repeated until there is no longer a soil moisture storage forecast in excess of the soil porosity, or the soil surface is reached. If the soil surface is reached, the excess soil moisture storage is added to the ponding depth (return flow), and is available for surface runoff if the ponding depth exceeds the depression storage. Surface runoff Q_s from each grid cell is allowed in any one of the eight directions, whichever is the maximum downslope direction, and is modeled using the Manning equation. The reader is referred to *Walker et al.* [2001b] for further details on the application of boundary conditions at the surface and base of the soil column.

3. Covariance Forecasting

[14] After algebraic manipulation of (7) we can obtain the linear state-space equation in the explicit form required for the KF covariance forecasting

$$\hat{\mathbf{X}}^{n+1/n} = \mathbf{A}^{n} \cdot \hat{\mathbf{X}}^{n/n} + \mathbf{U}^{n}, \quad (8)$$

where

$$\mathbf{A}^{n} = \left[\Phi_1^{n+1}\right]^{-1} \cdot \left[\Phi_2^{n}\right] \quad (9a)$$

$$\mathbf{U}^{n} = \left[\Phi_1^{n+1}\right]^{-1} \cdot \left[\Omega_2^{n} - \Omega_1^{n+1}\right]. \quad (9b)$$

The reader is referred to *Walker et al.* [2001a] for the KF forecasting and updating equations in the context of a one-dimensional problem.

[15] Once convergence of (7) has been achieved, the system state covariances may be forecast using the converged value for **A** from (9a). Using this approach, iteration is performed only for forecasting the system states, with evaluation of **A** and forecasting of the system state covariances performed only once (after convergence of the system states), using a single large time step. As forecasting of the system state covariance matrix is the most computationally demanding step of the KF, this approach minimizes the computational effort required to forecast the system states and the associated covariances. However, in our application the computation time for forecasting the covariance matrix was still very large. The reasons for this were: (1) evaluation of **A** using (9a) required inversion of Φ_1 and then multiplication by Φ_2, resulting in a nonsymmetric nonsparse matrix; and (2) forecasting of the covariances required a triple matrix product with rather large (720×720 in our application) nonsparse, nonbanded, nonsymmetric matrices. Hence, a computationally efficient procedure for forecasting the covariances is developed below. While an explicit model would limit some of the computational expense in covariance forecasting due to additional matrix multiplication and inversion, the time step size required to ensure stability made model operation impracticable.

3.1. Covariance Forecasting by the Modified Kalman Filter

[16] An example of state covariance forecasting by dynamics simplification is the simplified KF of *Dee* [1991]. The simplified KF predicts the forecast covariance evolution by a simplified version of the forecast model, unlike the KF in which the full forecast model is used for evaluation. Moreover, the contribution to forecast covariance evolution due to model error forcing is approximated only as a final step at the end of the forecast cycle.

[17] This paper takes a slightly different approach. As the magnitude of variances in the forecast covariance matrix using the KF is controlled primarily by the system noise covariance matrix **Q**, which is generally poorly estimated, we forecast only the correlation between system states. With a forecast correlation structure and estimated system state variances (for instance, a standard deviation equal to 5% of the state value), the forecast covariance matrix can be easily assembled. This is termed the modified Kalman filter (MKF) in this paper. If the essential aspects of the forecast system state dynamics can be captured by this simplified error model, the resulting loss of accuracy in estimating the forecast covariances should be acceptable, in view of the many other approximations and lack of information in the KF.

[18] Forecasting of the system state covariance matrix with the KF is performed by $\Sigma^{n+1} = \mathbf{A}\cdot\Sigma^{n}\cdot\mathbf{A}^{\mathrm{T}}$ (excluding the model error term). Thus the **A** matrix is obviously the driving force in forecasting the temporal (and spatial) evolution of the covariance matrix Σ, so we use just $\mathbf{A}\cdot\mathbf{A}^{\mathrm{T}}$ to estimate the temporal evolution of correlations between the states. However, the **A** matrix is rather noisy from one time step to the next, due to the nonlinearity in soil moisture modeling (particularly during infiltration events) and switching of sign from infiltration to exfiltration, thus an autoregressive smoothed value of **A** has been used to smooth the evaluation of $\mathbf{A}\cdot\mathbf{A}^{\mathrm{T}}$.

[19] Evaluating **A** at every time step using (9a) is in itself computationally demanding, as a result of the matrix inversion and multiplication. A much more efficient way of obtaining an autoregressive smoothed value of **A** is to evaluate the autoregressive smoothed values of Φ_1 and Φ_2 (used to compute **A**) by

$$\bar{\Phi}^{n+1} = \alpha\bar{\Phi}^{n} + (1-\alpha)\Phi^{n+1}, \tag{10}$$

where $\bar{\Phi}$ is the autoregressive smoothed Φ and α is a smoothing value close to 1. The autoregressive smoothed value of **A**, $\bar{\mathbf{A}}$, is then evaluated when required by

$$\overline{\mathbf{A}} = \left[\overline{\Phi}_1\right]^{-1}\left[\overline{\Phi}_2\right]. \tag{11}$$

The correlations ρ between states i and j are then estimated from

$$\Gamma = \overline{\mathbf{A}}\cdot\overline{\mathbf{A}}^{\mathrm{T}} \tag{12}$$

after scaling Γ to a "correlation" matrix (i.e. 1 on the diagonal by treating the unscaled Γ as if it were a variance-covariance matrix and dividing the "variances" by themselves and the "covariances" by their respective "standard deviations") by

$$\rho_{X_i,X_j} = \exp(\beta), \tag{13}$$

where

$$\beta = \left(1 - \frac{1}{(\Gamma_{i,j})^{a}}\right)\cdot b. \tag{14}$$

$\Gamma_{i,j}$ is the i,jth element of the scaled Γ, while a and b are empirical coefficients: when $\Gamma_{i,j}$ is 1 then β equals 0 and the correlation is 1; when $\Gamma_{i,j}$ is 0 then β equals $-\infty$ and the correlation is 0.

[20] In order to estimate the correlations between system states using the approach outlined above, it was necessary to evaluate appropriate values for the empirical coefficients α, a and b. This was achieved by calibrating the MKF to the original KF estimate of the correlations for a synthetic one-dimensional data set (soil type 1, Table 1). Soil type 1 represents a uniform clay profile.

[21] The coefficients α, a and b were satisfactorily calibrated as 0.995, 0.1, and 0.01, respectively (Figure 2a). The value of α equal to 0.995 was chosen as a compromise between noise in the correlation estimate during periods of lower correlation, correct modeling of the overall shape of the time evolution of correlation, and correct estimation of correlation during periods of high correlation. It can be noted that the correlation between the near-surface soil layer and the deeper soil layers was high when the soil profile was wet, and decreased as the soil profile dried. Moreover, this decrease in correlation with the near-surface layer increased with depth.

[22] To investigate whether the calibrated parameters were applicable for other soils, the correlations were estimated using both the MKF and KF for two different soil

Table 1. Initial Soil Moisture Values and Soil Parameters for Soil Moisture Profile Simulation

Soil Type	Layer	Thickness, mm	θ_I, % v/v	K_S, mm/h	ϕ, % v/v	θ_r, % v/v	n	*MGRAD*, mm
1	1	10	25	10.5	54	20	1.8	280
1	2	90	27	10.5	54	20	1.8	280
1	3	200	29	10.5	54	20	1.8	280
1	4	300	32	10.5	54	20	1.8	280
1	5	400	35	10.5	54	20	1.8	280
2	1	10	25	100	50	5	1.8	300
2	2	90	27	25	48	8	1.6	250
2	3	200	29	15	45	9	1.4	200
2	4	300	32	7	42	10	1.2	100
2	5	400	35	5	38	10	1.1	50
3	1	10	25	10.5	54	5	1.8	280
3	2	90	27	10.5	50	8	1.8	280
3	3	200	29	10.5	45	10	1.8	280
3	4	300	32	10.5	42	12	1.8	280
3	5	400	35	10.5	38	15	1.8	280

types (soil types 2 and 3, Table 1). Soil type 2 has a gradational soil profile with a sandy loam at the surface and clay at depth, while soil type 3 is a clay with uniform hydraulic conductivity, but depth varying soil porosity and residual soil moisture content.

[23] The time series of correlation associated with soil types 2 and 3 are given in Figures 2b and 2c. Figure 2b shows that correlations from the MKF are overpredicted relative to KF estimates by as much as about 0.2 for soil type 2, while Figure 2c shows that correlations from the MKF are underpredicted relative to KF estimates by only as much as about 0.05 for soil type 3 (neglecting the few spurious values).

[24] Given that the correlation between soil moisture in the near-surface soil layer and the deep soil layer during the dry period was so low (approximately 0.5) for soil type 2, the fact that the correlation was overpredicted by about 0.2 was not as important as it would be if the correlation was

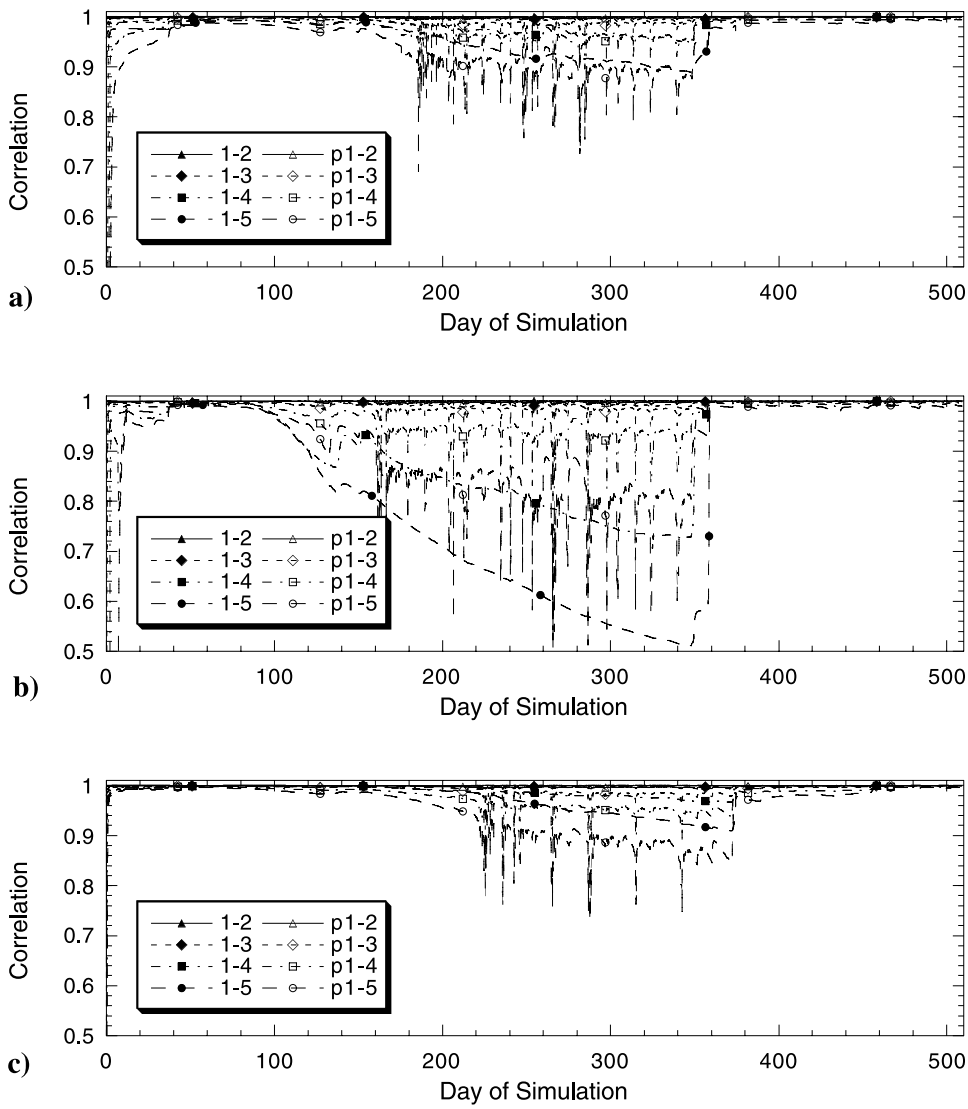

Figure 2. Comparison of the predicted (p) correlations (open symbols) using the MKF and KF estimate of correlations (solid symbols) between the near-surface soil layer (1) and soil layers 2 to 5 (i.e., p1-4 is the predicted correlation between soil layers 1 and 4) for (a) soil type 1, (b) soil type 2, and (c) soil type 3.

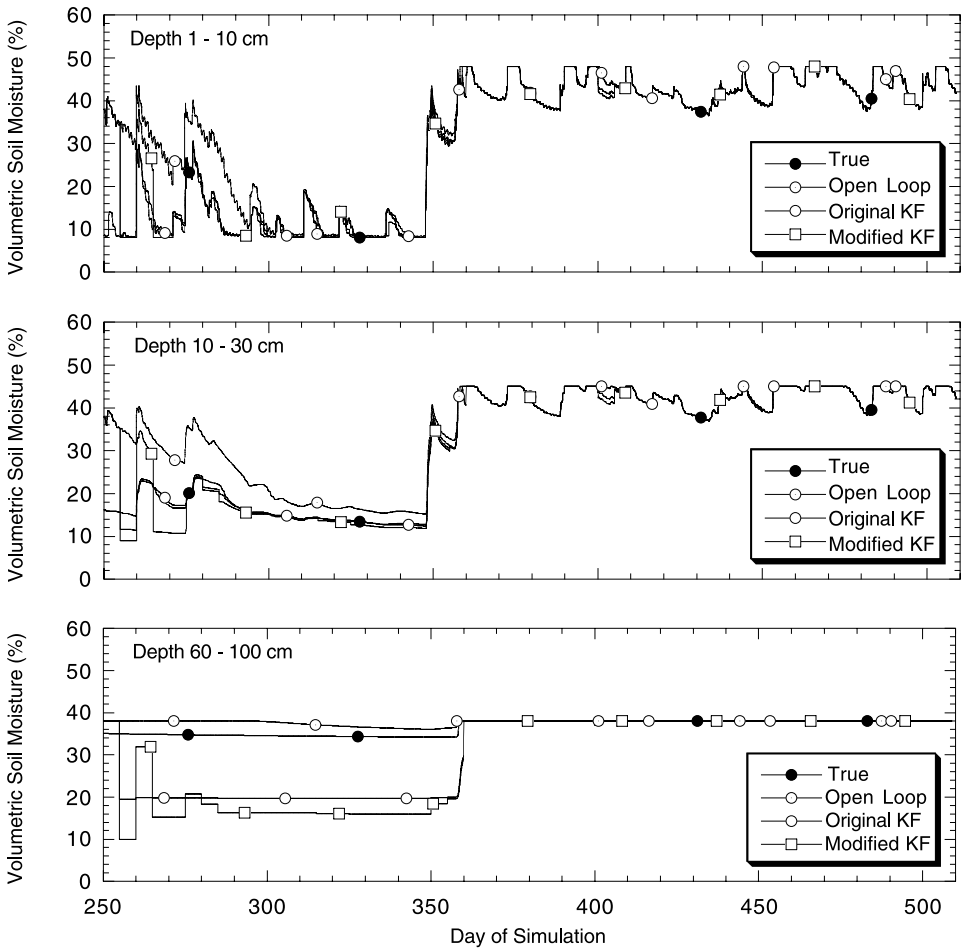

Figure 3. Comparison of soil moisture retrieval for soil type 2 using the MKF and KF assimilation schemes with near-surface soil moisture observations over 1 cm depth once every 5 days.

much closer to 1. The important point is that the approach predicted the strong correlations very well, and at least qualitatively tracked the decrease in correlation during the drying periods. Moreover, the KF is itself only an estimate of the correlations, being dependent on the initial correlations specified, linearization of the forecasting model, and the application of model noise. This limits us from making any quantitative comparison between the two approaches, as a poor agreement between correlations from the MKF and KF would not necessarily mean that correlations estimated from the MKF are poor, only that it is a poor approximation of the KF and its assumptions.

3.2. Evaluation of the Modified Kalman Filter

[25] The important issue is not how well the MKF can reproduce the correlations predicted by the KF, but rather the ability to make improvements to the forecasting of soil moisture profiles when using the MKF. To evaluate this, the MKF was applied to the synthetic one-dimensional soil column with soil type 2, and compared with true, open loop (i.e. no updating) and original KF simulations. Soil type 2 was used for this demonstration as it had resulted in the worst match between the MKF and the KF.

[26] The "true" soil moisture profiles are synthetic data generated from the one-dimensional model, while the open loop refers to the situation where no observations were used to update the soil moisture model. Synthetic data has been used, so that the MKF could be evaluated against the KF independent of the effects from model error on the retrieval of the true soil moisture profile. The MKF was only evaluated for a one-dimensional soil column due to computational constraints and the presumption of stronger correlations between soil layers than between grid cells. Nevertheless, the results from this investigation should be indicative of the results to be observed by application of the MKF to the spatially distributed problem.

[27] The aim of these simulations was to evaluate the MKF when the forecast correlations differed most from those of the KF, and the initialization of the soil moisture profile was poor. Hence, the simulations were commenced during the dry summer period when the prediction of correlations by MKF was comparatively poor. The retrieval and open loop simulations were initialized with a poor guess of 38% v/v uniform throughout the profile. The results from these simulations are given in Figure 3 and suggest that the MKF is a good approximation to the KF, despite differences in correlation forecasts.

[28] Simulations of the soil moisture profile for soil type 2 showed a poor retrieval of the soil moisture content at deeper soil layers during the dry period when using both the MKF and KF assimilation schemes. While the near-surface soil layers came on track with the true soil moisture content

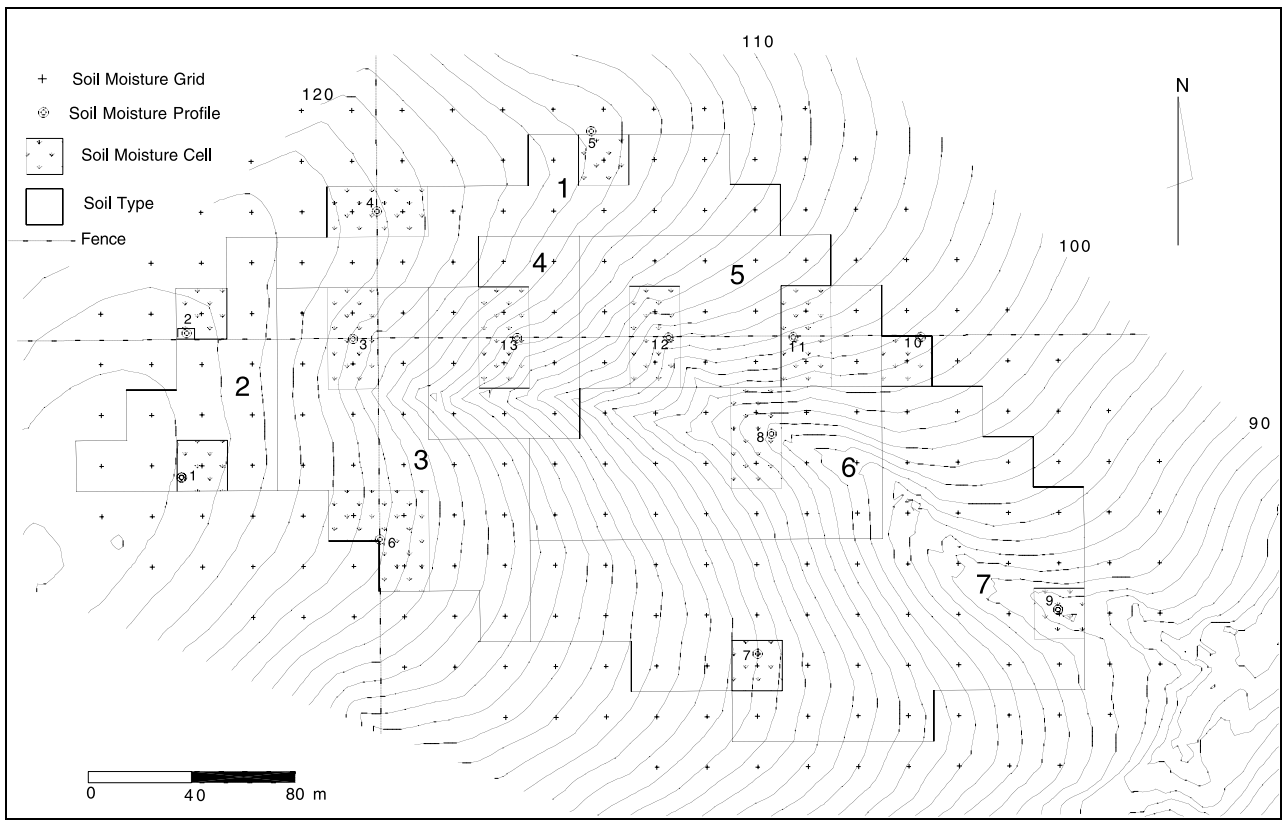

Figure 4. Plan of the Nerrigundah catchment showing the seven uniform soil type regions, 13 soil moisture profile monitoring sites, and the model grid cells used for comparison with soil moisture profile observations.

after only 1 update, the deeper soil layers were overcorrected in the first update, and did not come on track until the wetting up period. The reason for this was that soil moisture content in the top most observation layer followed the observed soil moisture content almost exactly, even though the soil moisture content of deeper soil layers was incorrect. This did not occur when the simulation was commenced during the wetter winter months, with the true profile being retrieved after 10 days (2 updates).

[29] The reason why no improvement was made in the deeper soil layers when the soil moisture model accurately forecast the near-surface soil moisture content may be seen from the KF update equation. The KF update equation adjusts the system state forecast by adding a correction term, which is the KF gain multiplied by the difference between the observations and the system state forecast, with the KF gain evaluated as a function of the observation and system state covariance matrices. Hence, if there is no discrepancy between the forecast system states and the observations, then the KF update equation cannot make any adjustment to the state forecast of deeper depths, irrespective of the assumptions made in evaluating the observation and system state covariance matrices, and hence KF gain.

[30] The phenomenon of decoupling between the near-surface soil moisture content and that of deeper soil layers has been observed in the field by *Capehart and Carlson* [1997], as a result of divergence between the drying rates at the surface and deeper levels. The significance of this is that when the near-surface soil layer becomes decoupled from the deep soil layers, the near-surface soil layer does not reflect the soil moisture status of deeper soil layers. Hence, under decoupled conditions, there can be no meaningful updating of the soil moisture profile once the near-surface soil layer correctly tracks the near-surface soil moisture content. This decoupling is indicated in Figure 2b by the low correlation between deeper soil layers and the near-surface soil layer.

[31] This phenomenon of decoupling suggests that if an update is performed too soon after initialization of the forecasting model and the associated covariance matrix, then the KF may update the near-surface soil layer correctly, but incorrectly for the deeper soil layers, as the forecast covariances are still affected by the initial conditions. If the near-surface layer and deep soil layers are decoupled, then estimation of the soil moisture profile will continue to be poor.

4. Field Data

[32] Having demonstrated the MKF on a one-dimensional case study, we now move to the three-dimensional field study. The field data used in this study is from the 6 ha "Nerrigundah" experimental catchment (Figure 4), located in a temperate region of eastern Australia. A detailed description of the entire data set is given by *Walker et al.* [2001c], so only the pertinent details are given here. The main objective of this rangeland experimental catchment was to enable a soil moisture assimilation study at the catchment scale.

4.1. Catchment Monitoring

[33] The Nerrigundah catchment was instrumented to monitor evapotranspiration, precipitation and soil moisture from 22 August 1997 to 20 October 1998, with an intensive soil moisture mapping campaign from 27 August 1997 to 22 September 1997. During the intensive field campaign, near-surface soil moisture measurements were made using 15 cm connector time domain reflectometry (TDR) probes on a 20 m $\times$ 20 m grid every 2 to 3 days, to replicate remote sensing observations. These near-surface soil moisture mappings were undertaken on a total of 12 days. The soil moisture profile was monitored at 13 locations throughout the catchment on the same days as near-surface measurements during the intensive field campaign, and on a less frequent basis at other times, to provide model evaluation and calibration data. Precipitation was monitored with two pluviometers and four collecting rain gauges to quantify spatial variability in precipitation across the catchment.

4.2. Soil Moisture Considerations

[34] Soil moisture variations at the 13 profile locations were monitored using connector TDR probes of nominal length 5, 10, 15, 20, 30, 40, 50, 60, 80 and 100 cm, to the lesser of 100 cm or bedrock. Comparison of connector TDR data with thermogravimetric measurements showed that the standard calibration was adequate for the 10 and 15 cm probe lengths, while the 5 cm probe lengths yielded a noisy response [*Walker*, 1999]. The calibration of longer TDR probes was not evaluated due to the destructive nature and labor intensiveness of the testing, the number of calibration data values required to make conclusive statements regarding accuracy, and the good agreement for the shorter probes. In addition, literature suggests that longer probes should not result in a further loss of accuracy.

[35] In modeling soil moisture content, it is necessary to have an idea of both the subgrid and intergrid variability in the system being modeled. For a grid resolution of 20 m, subgrid variability is the variability in soil moisture content over distances less than 10 m, while intergrid variability is the variability in soil moisture content over distances greater than 20 m.

[36] To investigate the subgrid variability, soil moisture measurements for 25 m transects (with measurements every 0.5 m) and 5 m transects (with measurements every 0.1 m) were assessed. Intergrid variability was estimated by assessing the differences between grid point measurements of soil moisture content from the soil moisture mappings on the different days. These results showed that apart from saturated conditions, the subgrid variability was approximately 1 to 2% v/v with a standard deviation of $\pm$1 to 2% v/v. This variability was constant within the $\pm$10 m, but started to increase for greater distances. Hence the subgrid variability was approximately that of the measuring device. The intergrid variability was approximately 5% v/v for a distance of 20 m and increased to approximately 10% v/v at a distance of 400 m, with a standard deviation of $\pm$5% v/v. This intergrid variability was more than double that of the subgrid variability, which would suggest that a grid resolution of 20 m was appropriate for the Nerrigundah catchment.

4.3. Soil Characterization

[37] The Nerrigundah soil was characterized by a combination of field and laboratory tests. Field tests included Guelph permeameter and double ring infiltrometer tests for saturated hydraulic conductivity, while laboratory tests on 19 minimally disturbed soil cores included the determination of soil depth, soil horizons, soil bulk density and porosity, and particle size analysis.

4.4. Evapotranspiration

[38] Actual evapotranspiration was estimated from Penman-Monteith potential evapotranspiration and a soil moisture stress index. The soil moisture stress index is used to limit the potential evapotranspiration rate as a function of the available water in the soil. The soil moisture stress index used in this study was the average column soil moisture content divided by the average column porosity. Measurements of actual evapotranspiration using the eddy correlation technique on 6 days were used to verify the linear soil moisture stress index used.

5. Field Application

[39] In this section, the distributed soil moisture model is calibrated and evaluated against the soil moisture profile measurements made in the Nerrigundah catchment. The calibrated model is then used for retrieval of the soil moisture profile by assimilation of the near-surface soil moisture measurements using the MKF.

5.1. Calibration of Model

[40] The soil moisture profile measurements provided the data for calibration and evaluation of the soil moisture forecasting model. As the soil moisture model was to be applied to data collected during the intensive field campaign, calibration of the model was performed for the period following this campaign (14 October 1997 to 22 July 1998). Thus the forecasting model was calibrated to data that was independent of that used for soil moisture profile retrieval.

5.1.1. Observed Model Parameters

[41] During model calibration, both residual soil moisture content and soil porosity were inferred from soil moisture measurements at the 13 soil moisture profiles. Soil porosity was also inferred from laboratory tests on the 19 soil cores. Other parameters, such as total soil depth, saturated hydraulic conductivity and depression storage (5 mm), were inferred from field measurements. A Manning's n value of 0.2 [*Streeter and Wylie*, 1983] was used as representative for rangeland. The only parameters requiring calibration were the maximum gradient parameter *MGRAD* and the van Genuchten soil parameter n. The model assumed isotropy within each grid element but allowed different parameters for each individual grid element. The calibration period was initialized with soil moisture values interpolated from the soil moisture profile measurements made on 14 October 1997.

[42] To reduce the number of soil parameters to be estimated, the Nerrigundah catchment was divided into a number of ''uniform'' soil type regions (Figure 4). These regions had different soil properties in each model layer, but the same layer properties for each grid cell within the uniform soil type region. Delineation of the regions was based on soil porosity, residual soil moisture content and saturated hydraulic conductivity within the four soil horizons. Model layer thicknesses were defined from observed soil horizon thicknesses as a proportion of the total soil depth.

Table 2. Soil Properties Used for the Seven Uniform Soil Type Areas

Soil Type	Soil Horizon	ϕ, % v/v	θ_r, % v/v	K_S, mm/h	*MGRAD*, mm	*n*
1	A1	50	5	80	340	2.1
1	A2	46	7	20	70	1.2
1	B1	32	8	5	15	1.8
1	B2	32	10	0.5	350	2.0
2	A1	60	6	35	490	2.5
2	A2	45	8	10	400	1.9
2	B1	42	12	3	145	2.0
2	B2	40	15	1	50	1.9
3	A1	60	4	25	315	2.3
3	A2	54	4	20	58	1.6
3	B1	38	4	15	40	2.0
3	B2	36	6	5	130	2.1
4	A1	50	9	30	497	2.4
4	A2	47	9	5	9	2.5
4	B1	42	9	3	119	1.2
4	B2	31	11	1	34	2.0
5	A1	50	60	5	320	2.4
5	A2	46	50	6	245	1.5
5	B1	32	38	10	260	1.3
5	B2	32	38	18	360	1.5
6	A1	60	10	15	500	2.5
6	A2	37	13	3	104	1.2
6	B1	34	16	1	2	1.4
6	B2	32	20	0.5	88	2.5
7	A1	60	6	35	500	2.5
7	A2	46	8	15	1	1.7
7	B1	44	9	2	375	1.3
7	B2	34	16	0.1	320	2.0

5.1.2. Calibrated Model Parameters

[43] Calibration of the three-dimensional model was undertaken using a series of one-dimensional calibrations. Each of the 13 soil moisture monitoring sites was considered as an independent one-dimensional soil profile, and the unknown soil parameters calibrated independently. Simulated soil moisture contents were fitted to the connector TDR depth integrated soil moisture measurements for various depths using the Bayesian nonlinear regression program NLFIT. The program suite NLFIT [*Kuczera*, 1994] is an interactive optimization package, employing the SCE-UA (Shuffled Complex Evolution Method developed at the University of Arizona) of *Duan et al.* [1994]. This approach implicitly assumes that the effects from lateral redistribution were negligible relative to vertical redistribution. Apart from soil moisture profiles located in the main drainage lines and steeper sections of the catchment, this assumption was found to be valid, with very little difference displayed between one-dimensional and three-dimensional simulation results. As soil moisture measurements with the 5 cm connector TDR probes had a wide range of variation when compared with thermogravimetric measurements, calibration was only performed for soil moisture measurements of horizons A1 and A2, A1 to B1 and A1 to B2 (i.e. model layers 1 to 3, 1 to 4 and 1 to 5). The averaged soil parameters assigned to each of the uniform soil type areas are given in Table 2.

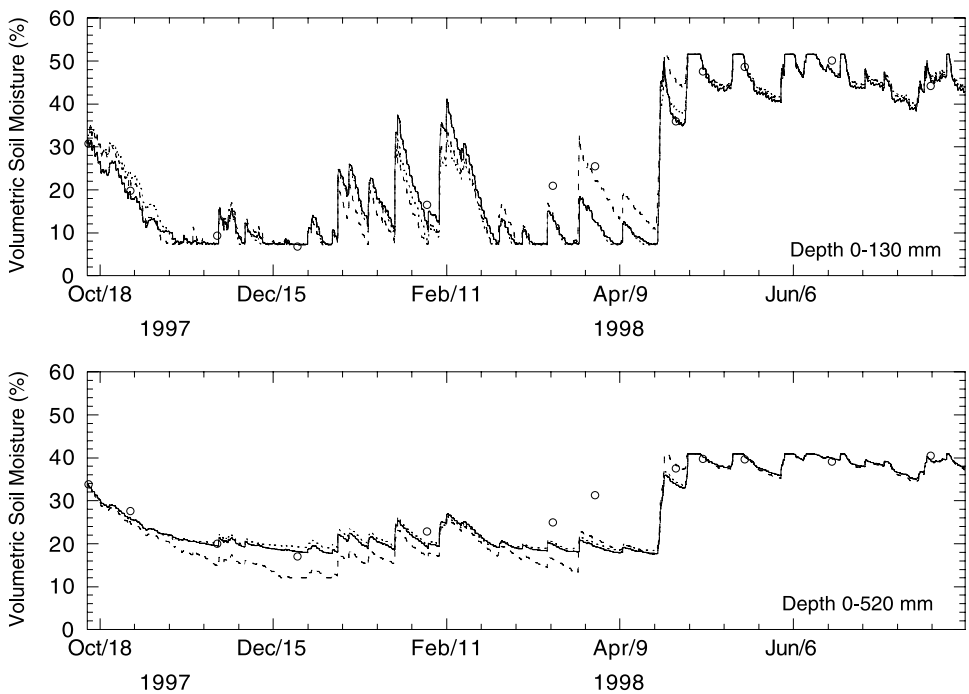

Figure 5. Calibration results from profile 7. Connector TDR observations (open circles) are compared against one-dimensional simulation results with calibrated parameters (solid line) and averaged parameters (short-dashed line), and three-dimensional simulation results with averaged parameters (long-dashed line). The difference between the solid line and the short dashed line is the effect of averaging calibrated soil parameters for the uniform soil type, while the difference between short dashed and long dashed lines is the effect of lateral redistribution.

[44] Figure 5 shows a comparison of calibration results and data at profile 7. This profile was typical of the results from other profiles, with midrange soil depth (520 mm) and a midslope location. In Figure 5, simulation results from the one-dimensional model using the calibrated parameters are compared with results from the one-dimensional model using the averaged soil parameters (for uniform soil type regions containing more than one soil moisture profile), and results from the three-dimensional model. There is only a slight difference between the three simulations, and a very good agreement with the observations, particularly for deeper depths.

[45] The good agreement between one-dimensional simulations when using both the calibrated and averaged soil parameters, indicated that averaging of the soil moisture profile monitoring site calibrations within a uniform soil type area had a minimal impact on the calibration of the one-dimensional model. Moreover, the good agreement between the one-dimensional and three-dimensional simulations indicates that neglecting the lateral redistribution of soil moisture in the model calibration had a minimal impact on the calibration results. The implication of this is that vertical redistribution was more important than lateral redistribution in the Nerrigundah catchment.

5.2. Soil Moisture Profile Retrieval

[46] The ability to retrieve the spatial and temporal variation of soil moisture profiles from near-surface soil moisture measurements under field conditions using the MKF assimilation scheme was evaluated during the period of the intensive field campaign; 22 August to 22 September 1997. Soil moisture profile observations were made at all profile monitoring sites on 22 August, but observations of near-surface soil moisture were not made until 27 August. Hence updating of the forecasting model could not commence until 27 August. Near-surface soil moisture observations on 19 September were not used for updating of the model, due to the rainfall that fell during that day. However, these latter soil moisture profile observations are presented for comparison with the model output of soil moisture.

[47] The near-surface soil moisture observations used were the 15 cm connector TDR measurements on the 20 m $\times$ 20 m grid. The 15 cm connector TDR observations of near-surface soil moisture content have been applied as observations of the top 15 cm of the soil profile, as it is important that the near-surface soil moisture observations be applied to the depth for which they relate. However, results from updating with an observation depth of 15 cm can be considered indicative of the results that would be obtained from observations over a much shallower depth, as *Walker et al.* [2001a] have illustrated that one-dimensional soil moisture profile retrieval with the KF was insensitive to the near-surface soil moisture observation depth. In updating the forecast model, a system state standard deviation of 5% v/v, based on observed model fit to data during the model evaluation period (Table 3, case I), and an observation error of 2% v/v for the near-surface soil moisture observation, based on an estimate of instrument error and subgrid variability from field measurements, were used.

[48] Five cases were examined: (1) measured initial soil moisture profile with no updating; (2) poor initial guess of the soil moisture profile with no updating; (3) poor initial guess of the soil moisture profile with updating every few days; (4) measured initial soil moisture profile with updating every few days; and (5) poor initial guess of the soil moisture profile with only the first update.

Table 3. Comparison of Minimum, Mean, and Maximum RMS Errors in Soil Moisture Across All Profile Monitoring Sites From 27 August Until 22 September

	Soil Horizons, % v/v			
Scenario	A1	A1–A2	A1–B1	A1–B2
Case I	2.8, 9.6, 20.2	2.2, 5.9, 13.4	1.6, 4.6, 11.0	1.1, 4.3, 6.2
Case II	5.3, 20.8, 29.0	5.5, 15.8, 26.2	3.7, 14.2, 22.8	4.7, 13.4, 19.8
Case III	5.1, 9.3, 17.2	3.5, 7.9, 11.6	4.7, 6.7, 10.1	3.9, 6.2, 10.8
Case IV	4.0, 9.1, 17.5	4.1, 7.7, 11.1	4.1, 6.4, 8.5	3.3, 6.3, 9.1
Case V	3.9, 9.4, 15.0	3.7, 7.5, 12.5	3.6, 6.4, 11.2	2.0, 6.1, 11.8

5.2.1. Case I

[49] Results from the evaluation of the model calibration are given in Figure 6 for profile 7, with a good agreement between the model and observations. This is a true test of the model and its calibration as this data was not used during the model calibration. Initial soil moisture values were interpolated between the 13 profile measurements made on 22 August 1997. While there was only a limited range of soil moisture contents during this test period, the evaluation confirms that the calibration was adequate for forecasting the soil moisture profiles. The RMS errors were generally less than about 5% v/v for all profiles (see Table 3). Simulation of soil moisture content in the A1 horizon had the highest RMS error, believed to result from the noisy observations using the 5 cm connector TDR probes. Profile 12 had the largest RMS error across all depths (see maximum values in Table 3). This is a result of the monitoring site being located in a depression but, due to the grid resolution, is not identified as such in the model (see Figure 4).

5.2.2. Case II

[50] A simulation was performed for a poor guess of the initial soil moisture on 22 August 1997, being 12, 15, 18 and 20% v/v for the A1, A2, B1 and B2 soil horizons respectively, uniform across the catchment. A comparison of the results from this simulation with field measurements is given in Figure 7 for profile 7. The RMS errors for this simulation were much greater than for case I; around 15% v/v for all profiles (Table 3). This was to be expected given the poor initial conditions used.

5.2.3. Case III

[51] This simulation used the same poor initial conditions as case II, but assimilated the near-surface soil moisture observations using the MKF. A comparison of the results from this simulation with field measurements is also given in Figure 7 for profile 7, where an obvious improvement can be seen in the retrieved soil moisture profile compared to case II, the open loop simulation. The RMS errors for this simulation were reduced to around 7% v/v for all profiles (Table 3). This highlights the obvious benefit that may be obtained from assimilating near-surface soil moisture observations into the forecasting model. A comparison of cases I and III (see Table 3) would suggest that initialization of the forecast model is not an important aspect of the soil moisture profile retrieval algorithm when using the MKF

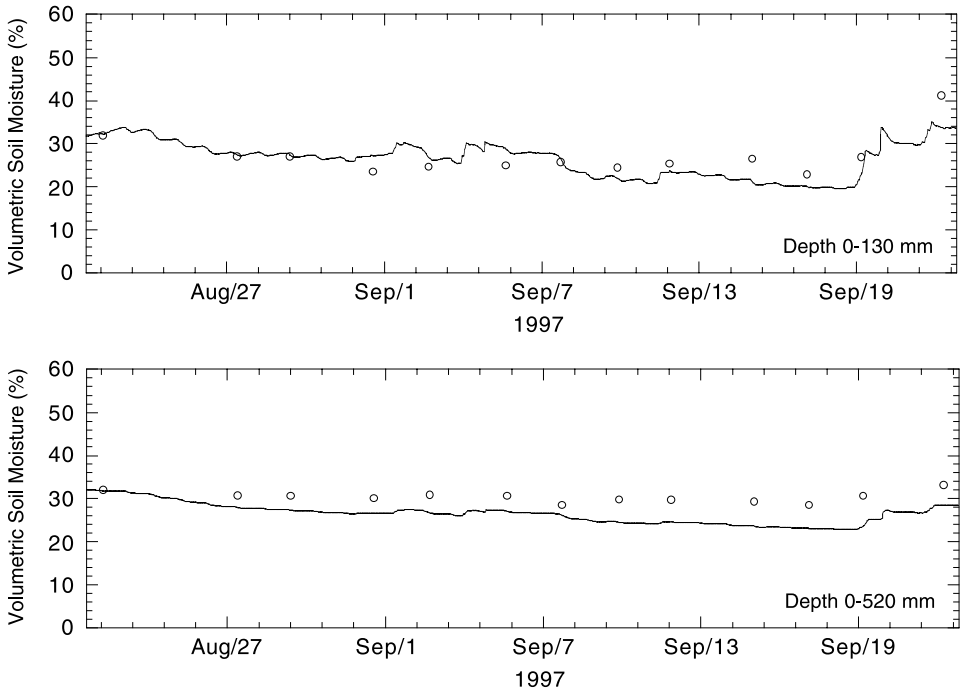

Figure 6. Evaluation of soil moisture simulation at profile 7 during the intensive field campaign. Connector TDR observations (open circles) are compared against three-dimensional simulation results with calibrated parameters (solid line).

assimilation scheme, with RMS errors being only about 2% v/v greater than for case I.

[52] Figure 7 shows that the MKF actually degraded the retrieved soil moisture profile at some update times when compared with measurements. We believe that this was a result of lateral correlations in the update, as a result of model predictions for adjacent grid cells having a poor comparison with the near-surface soil moisture observations. Furthermore, simulation results have suggested that when near-surface soil moisture observations are of low quality, and this is not reflected by the observation variances, the soil moisture profile retrieval may be poor. Hence,

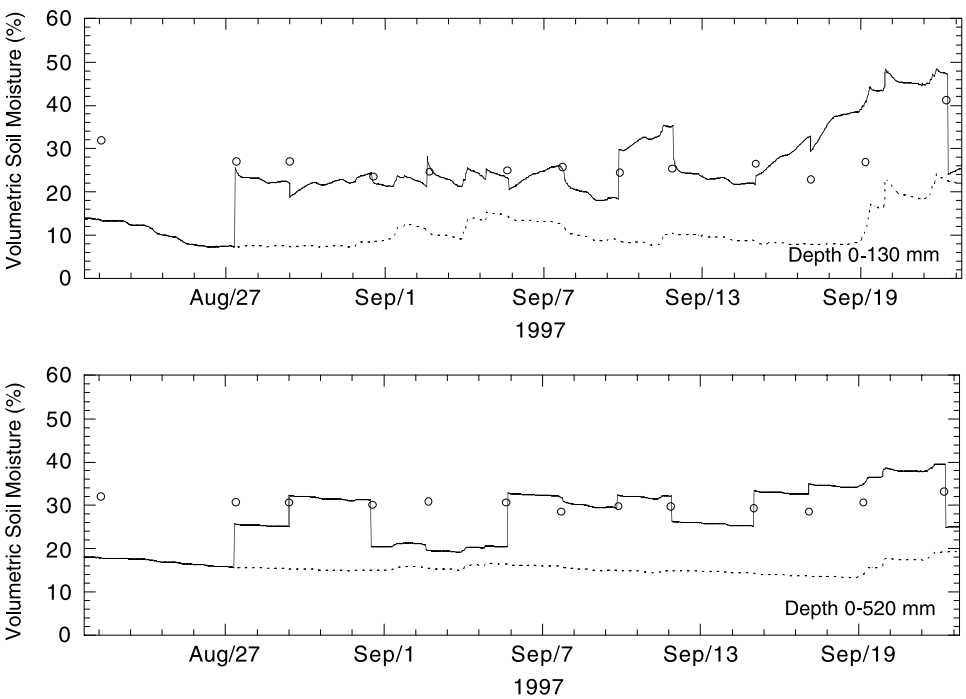

Figure 7. Evaluation of soil moisture retrieval at profile 7. Connector TDR observations (open circles) are compared against the retrieved soil moisture profile (solid line) and open loop simulation results (dashed line) for simulations with a poor initial guess of the soil moisture content.

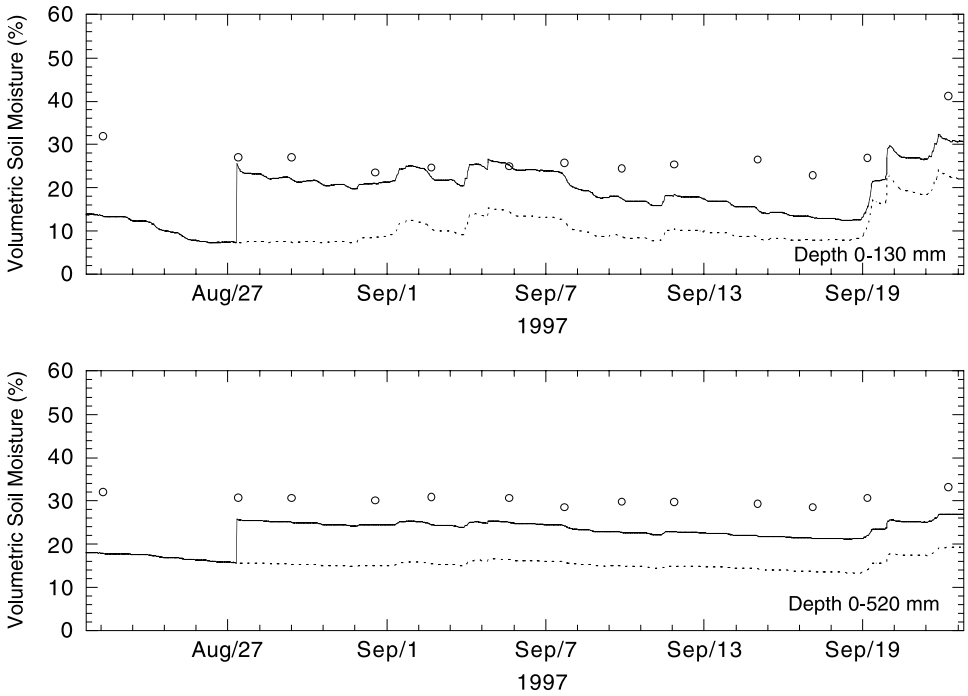

Figure 8. Same as Figure 7 but only the first set of near-surface soil moisture observations are used in the soil moisture profile retrieval.

updates for these times may be improved by using a non-constant system state variance and a spatially uniform observation error. Moreover, there is the difficulty of relating point measurements to the spatially averaged estimates from a soil moisture model.

5.2.4. Case IV

[53] This is the same as for case III, with the exception that the initial soil moisture values used were the same as those for case I. When comparing the RMS errors from case III and case IV (Table 3), there is perhaps a very slight improvement for this simulation. This would again suggest that initialization of the forecast model is not an important aspect of the soil moisture profile retrieval algorithm when using the MKF assimilation scheme. It may also be seen from a comparison of the RMS errors for cases I and IV (Table 3) that when the forecast model was initialized with an accurate estimate of the soil moisture profile, soil moisture profile retrieval using the MKF was slightly degraded from the open loop simulation (approximately 2% v/v). The conclusion that may be drawn from this is that assimilation yields an improved estimate of the soil moisture profile when simulation results are poor, while only slightly degrading the soil moisture profile estimation when simulation results are good.

5.2.5. Case V

[54] To evaluate the effect of update frequency on soil moisture profile retrieval, the simulation with a poor guess of initial soil moisture was run with only the first set of near-surface soil moisture observations used for updating. Figure 8 shows a clear improvement in the profile retrieval when compared with the open loop simulation (case II). Furthermore, simulation results are comparable (see Table 3) to the results when all data are assimilated (case III). Thus updating interval is relatively unimportant for correct retrieval of the soil moisture profile when there is accurate model forcing data and a good calibration of the model, and where poor simulation of soil moisture profiles is solely a result of a poor initialization of the forecasting model. When the model is poorly calibrated or there are substantial errors in the forcing data, we believe correct estimation of the soil moisture profile will be more dependent on the updating interval.

6. Conclusions

[55] The single most difficult operation in applying the Kalman Filter (KF) to the spatially distributed assimilation problem is the computation time required for forecasting of the model covariance matrix. Moreover, a full-fledged application of the extended KF is, at best, a crude approximation to the actual forecast covariance matrix, as a result of model linearization errors, lack of statistics concerning model error, and the initial system state covariances. In overcoming the computational limitations of the KF assimilation scheme, a modified KF (MKF) was developed, based on simplified covariance forecasting techniques. The MKF forecasts the system state covariances through a dynamics simplification approach. Using this approach, the system state correlations are estimated from the dynamics of the forecast model and the covariances assembled at update times using specified system state variances. Simulations using both the MKF and KF have shown good agreement between the forecasting of correlations by the two filters. Despite differences in forecast correlation between the system states, the MKF predicted the higher correlations adequately and qualitatively tracked the decrease in correlation during drying periods, with a significant decrease in computational effort.

[56] Simulations of soil moisture profile retrieval using both the KF and MKF assimilation schemes showed that the

MKF performed as well as the KF, despite specifying the system state variances and differences in correlation forecasts between the two approaches. Moreover, these simulations showed that when the near-surface soil layer becomes decoupled from the deep soil layer the soil moisture profile cannot be retrieved. This decoupling occurs during extended drying periods as a result of a divergence between the drying rates at the soil surface and deeper levels. Thus during extreme drying events the KF (and its variants) is likely to perform poorly.

[57] Application of the MKF assimilation scheme to the Nerrigundah catchment showed that soil moisture profile estimates are degraded slightly (average RMS error increase of 2% v/v for the total soil moisture storage) if simulation and observation values are already close, as a result of noise in the near-surface soil moisture observations and spurious lateral correlations. However, when the simulation of the soil moisture profile is poor, assimilation of near-surface soil moisture into the forecasting model will make a significant improvement in the soil moisture profile estimation (average RMS error decrease of 7% v/v for the total soil moisture storage). This means that assimilation of near-surface soil moisture into the forecasting model will provide an improved estimate of the soil moisture profile on average for all simulation times.

[58] This study has also shown that, when using the MKF assimilation scheme, initialization of the model states was not important for adequate retrieval of the spatial distribution of soil moisture profiles. Moreover, it has been shown that the updating interval is relatively unimportant for correct retrieval of the soil moisture profile when the forecasting model has a good calibration and forcing data has a high level of accuracy. When model calibration is poor and/or there are significant errors in the model forcing data, the adequacy of soil moisture profile retrieval from low temporal resolution near-surface soil moisture measurements will be a function of the timescale over which the dynamics of the forecasting model cause a departure from the true soil moisture profile.

[59] **Acknowledgments.** This work has been jointly funded by an Australian Postgraduate Award scholarship and the Hunter Water Corporation. Assistance with field work was provided by Lyndon Bell, Greg Hancock, André Kable, Michael Kendal, Andrew Krause, Hemantha Perera, Rodger Grayson, Mark Scanlan, Mark Thyer, Wendy Walker, Andrew Western, Craig Wood and Scott Wooldridge. John and Margaret Russell are acknowledged for the use of their land in the monitoring of soil moisture.

References

Capehart, W. J., and T. N. Carlson, Decoupling of surface and near-surface soil water content: A remote sensing perspective, *Water Resources Research*, *33*(6), 1383–1395, 1997.

Dee, D. P., Simplification of the Kalman filter for meteorological data assimilation, *Q. J. R. Meteorol. Soc.*, *117*, 365–384, 1991.

Dee, D. P., On-line estimation of error covariance parameters for atmospheric data assimilation, *Mon. Weather Rev.*, *123*, 1128–1145, 1995.

Duan, Q., S. Sorooshian, and V. K. Gupta, Optimal use of the SCE-UA global optimization method for calibrating watershed models, *J. Hydrol.*, *158*, 265–284, 1994.

Entekhabi, D., H. Nakumara, and E. G. Njoku, Solving the inverse problem for soil moisture and temperature profiles by sequential assimilation of multifrequency remotely sensed observations, *IEEE Trans. Geosci. Remote Sen.*, *32*(2), 438–448, 1994.

Galantowicz, J., D. Entekhabi, and E. Njoku, Tests of sequential data assimilation for retrieving profile soil moisture and temperature from observed L-band radiobrightness, *IEEE Trans. Geosci. Remote Sens.*, *37*(4), 1860–1870, 1999.

Gerald, C. F., and P. O. Wheatley, *Applied Numerical Analysis*, 4th ed., Addison-Wesley-Longman, Reading, Mass., 1989.

Hoeben, R., and P. A. Troch, Assimilation of active microwave observation data for soil moisture profile estimation, *Water Resour. Res.*, *36*(10), 2805–2819, 2000.

Kuczera, G., NLFIT: A Bayesian Nonlinear Regression Program Suite, Dep. of Civ. Eng. and Surv., Univ. of Newcastle, Callaghan, Australia, 1994.

Reichle, R. H., D. B. McLaughlin, and D. Entekhabi, Hydrologic data assimilation with the ensemble Kalman filter, *Mon. Weather Rev.*, *130*(1), 103–114, 2002.

Streeter, V. L., and E. B. Wylie, *Fluid Mechanics*, 1st SI ed., McGraw-Hill, New York, 1983.

Todling, R., and S. E. Cohn, Suboptimal schemes for atmospheric data assimilation based on the Kalman filter, *Mon. Weather Rev.*, *122*, 2530–2557, 1994.

Walker, J. P., Estimating Soil moisture profile dynamics from near-surface soil moisture measurements and standard meteorological data, Ph.D. thesis, Dep. of Civ., Surv. and Environ. Eng., Univ. of Newcastle, Callaghan, Australia, 1999.

Walker, J. P., and P. R. Houser, A methodology for initializing soil moisture in a global climate model: Assimilation of near-surface soil moisture observations, *J. Geophys. Res.*, *106*(D11), 11,761–11,774, 2001.

Walker, J. P., P. A. Troch, M. Mancini, G. R. Willgoose, and J. D. Kalma, Profile soil moisture estimation using the modified IEM, in *Proceedings International Geoscience and Remote Sensing Symposium (IGARSS)*, edited by T. Stein, pp. 1263–1265, IEEE Press, Piscataway, N. J., 1997.

Walker, J. P., G. R. Willgoose, and J. D. Kalma, One-dimensional soil moisture profile retrieval by assimilation of near-surface observations: A comparison of retrieval algorithms, *Adv. Water Resour.*, *24*(6), 631–650, 2001a.

Walker, J. P., G. R. Willgoose, and J. D. Kalma, One-dimensional soil moisture profile retrieval by assimilation of near-surface measurements: A simplified soil moisture model and field application, *J. Hydrometeorol.*, *2*(4), 356–373, 2001b.

Walker, J. P., G. R. Willgoose, and J. D. Kalma, The Nerrigundah data set: Soil moisture patterns, soil characteristics and hydrological flux measurements, *Water Resour. Res.*, *37*(11), 2653–2658, 2001c.

J. D. Kalma and G. R. Willgoose, Department of Civil, Surveying and Environmental Engineering, University of Newcastle, Callaghan, New South Wales 2308, Australia.

J. P. Walker, Department of Civil and Environmental Engineering, University of Melbourne, Parkville, Victoria 3010, Australia. (j.walker@unimelb.edu.au)